

AD-A107 864

MASSACHUSETTS INST OF TECH CAMBRIDGE DEPT OF MATERIA--ETC F/6 20/2
ELECTRONIC STRUCTURE OF GRAIN BOUNDARIES AND INTERFACES IN POLY--ETC(U)
NOV 81 M H SUKKAR, H L TULLER, K H JOHNSON N00014-81-K-0899

UNCLASSIFIED

TR-2

NL

1 OF 1
AD-A
07864



END
DATE
FILMED
11-82
DTIC

UNCLASSIFIED

SECURITY CLASSIFICATION OF THIS PAGE (When Data Entered) **UNCLASSIFIED**

REPORT DOCUMENTATION PAGE		READ INSTRUCTIONS BEFORE COMPLETING FORM
1. REPORT NUMBER 2	2. GOVT ACCESSION NO. AD-A107864	3. RECIPIENT'S CATALOG NUMBER
4. TITLE (and Subtitle) Electronic Structure of Grain Boundaries and Interfaces in Polycrystalline Zinc Oxide		5. TYPE OF REPORT & PERIOD COVERED Interim
7. AUTHOR(s) M. H. Sukkar, H. L. Tuller, and K. H. Johnson		6. PERFORMING ORG. REPORT NUMBER
9. PERFORMING ORGANIZATION NAME AND ADDRESS Department of Materials Science and Engineering, M.I.T., Cambridge, Massachusetts		8. CONTRACT OR GRANT NUMBER(s) N00014-81-K-0499
11. CONTROLLING OFFICE NAME AND ADDRESS Office of Naval Research Department of the Navy Arlington, Virginia 22217		10. PROGRAM ELEMENT, PROJECT, TASK AREA & WORK UNIT NUMBERS Task No. NR 056-757
14. MONITORING AGENCY NAME & ADDRESS (if different from Controlling Office)		12. REPORT DATE November 18, 1981
		13. NUMBER OF PAGES
		15. SECURITY CLASS. (of this report)
		15a. DECLASSIFICATION/DOWNGRADING SCHEDULE
16. DISTRIBUTION STATEMENT (of this Report) Approval for public release; distribution unlimited.		
17. DISTRIBUTION STATEMENT (of the abstract entered in Block 20, if different from Report) DTIC ELECTE NOV 27 1981 A		
18. SUPPLEMENTARY NOTES		
19. KEY WORDS (Continue on reverse side if necessary and identify by block number) Electronic structures; grain boundaries; polycrystalline; zinc oxide.		
20. ABSTRACT (Continue on reverse side if necessary and identify by block number) Preliminary theoretical models for the electronic structure of grain boundaries and interfaces in polycrystalline ZnO have been constructed on the basis of self-consistent-field X-alpha scattered-wave (SCF-X _α -SW) cluster molecular-orbital calculations. The disposition and character of the interface states, relative to the valence and conduction bands of the otherwise perfect crystalline material, have been studied for clusters representing coordinatively unsaturated Zn surface sites and molecular O ₂ chemisorption		

DD FORM 1 JAN 73 1473

EDITION OF 1 NOV 65 IS OBSOLETE
S/N 0102-LF-014-6601

Unclassified

SECURITY CLASSIFICATION OF THIS PAGE (When Data Entered)

81 11 24 166

AD A107864

DTIC FILE COPY

UNCLASSIFIED

SECURITY CLASSIFICATION OF THIS PAGE (When Data Entered)

thereon. The possible effects of the resulting interface states on electron transport at grain boundaries in ZnO varistors have been addressed.

UNCLASSIFIED

SECURITY CLASSIFICATION OF THIS PAGE (When Data Entered)

OFFICE OF NAVAL RESEARCH

Contract N00014-81-K-0499

Task No. NR 056-757

TECHNICAL REPORT NO. 2

Electronic Structure of Grain Boundaries and Interfaces in Polycrystalline
Zinc Oxide

by

M. H. Sukkar, H. L. Tuller, and K. H. Johnson

Department of Materials Science and Engineering

Massachusetts Institute of Technology

Cambridge, Massachusetts 02139

November 18, 1981

Reproduction in whole or in part is permitted for
any purpose of the United States Government
Approved for Public Release: Distribution Unlimited

1. <input checked="" type="checkbox"/> Approved for Release	
2. <input type="checkbox"/> Not Approved for Release	
3. <input type="checkbox"/> Not Approved for Release	
4. <input type="checkbox"/> Not Approved for Release	
5. <input type="checkbox"/> Not Approved for Release	
6. <input type="checkbox"/> Not Approved for Release	
7. <input type="checkbox"/> Not Approved for Release	
8. <input type="checkbox"/> Not Approved for Release	
9. <input type="checkbox"/> Not Approved for Release	
10. <input type="checkbox"/> Not Approved for Release	
11. <input type="checkbox"/> Not Approved for Release	
12. <input type="checkbox"/> Not Approved for Release	
13. <input type="checkbox"/> Not Approved for Release	
14. <input type="checkbox"/> Not Approved for Release	
15. <input type="checkbox"/> Not Approved for Release	
16. <input type="checkbox"/> Not Approved for Release	
17. <input type="checkbox"/> Not Approved for Release	
18. <input type="checkbox"/> Not Approved for Release	
19. <input type="checkbox"/> Not Approved for Release	
20. <input type="checkbox"/> Not Approved for Release	
21. <input type="checkbox"/> Not Approved for Release	
22. <input type="checkbox"/> Not Approved for Release	
23. <input type="checkbox"/> Not Approved for Release	
24. <input type="checkbox"/> Not Approved for Release	
25. <input type="checkbox"/> Not Approved for Release	
26. <input type="checkbox"/> Not Approved for Release	
27. <input type="checkbox"/> Not Approved for Release	
28. <input type="checkbox"/> Not Approved for Release	
29. <input type="checkbox"/> Not Approved for Release	
30. <input type="checkbox"/> Not Approved for Release	
31. <input type="checkbox"/> Not Approved for Release	
32. <input type="checkbox"/> Not Approved for Release	
33. <input type="checkbox"/> Not Approved for Release	
34. <input type="checkbox"/> Not Approved for Release	
35. <input type="checkbox"/> Not Approved for Release	
36. <input type="checkbox"/> Not Approved for Release	
37. <input type="checkbox"/> Not Approved for Release	
38. <input type="checkbox"/> Not Approved for Release	
39. <input type="checkbox"/> Not Approved for Release	
40. <input type="checkbox"/> Not Approved for Release	
41. <input type="checkbox"/> Not Approved for Release	
42. <input type="checkbox"/> Not Approved for Release	
43. <input type="checkbox"/> Not Approved for Release	
44. <input type="checkbox"/> Not Approved for Release	
45. <input type="checkbox"/> Not Approved for Release	
46. <input type="checkbox"/> Not Approved for Release	
47. <input type="checkbox"/> Not Approved for Release	
48. <input type="checkbox"/> Not Approved for Release	
49. <input type="checkbox"/> Not Approved for Release	
50. <input type="checkbox"/> Not Approved for Release	
51. <input type="checkbox"/> Not Approved for Release	
52. <input type="checkbox"/> Not Approved for Release	
53. <input type="checkbox"/> Not Approved for Release	
54. <input type="checkbox"/> Not Approved for Release	
55. <input type="checkbox"/> Not Approved for Release	
56. <input type="checkbox"/> Not Approved for Release	
57. <input type="checkbox"/> Not Approved for Release	
58. <input type="checkbox"/> Not Approved for Release	
59. <input type="checkbox"/> Not Approved for Release	
60. <input type="checkbox"/> Not Approved for Release	
61. <input type="checkbox"/> Not Approved for Release	
62. <input type="checkbox"/> Not Approved for Release	
63. <input type="checkbox"/> Not Approved for Release	
64. <input type="checkbox"/> Not Approved for Release	
65. <input type="checkbox"/> Not Approved for Release	
66. <input type="checkbox"/> Not Approved for Release	
67. <input type="checkbox"/> Not Approved for Release	
68. <input type="checkbox"/> Not Approved for Release	
69. <input type="checkbox"/> Not Approved for Release	
70. <input type="checkbox"/> Not Approved for Release	
71. <input type="checkbox"/> Not Approved for Release	
72. <input type="checkbox"/> Not Approved for Release	
73. <input type="checkbox"/> Not Approved for Release	
74. <input type="checkbox"/> Not Approved for Release	
75. <input type="checkbox"/> Not Approved for Release	
76. <input type="checkbox"/> Not Approved for Release	
77. <input type="checkbox"/> Not Approved for Release	
78. <input type="checkbox"/> Not Approved for Release	
79. <input type="checkbox"/> Not Approved for Release	
80. <input type="checkbox"/> Not Approved for Release	
81. <input type="checkbox"/> Not Approved for Release	
82. <input type="checkbox"/> Not Approved for Release	
83. <input type="checkbox"/> Not Approved for Release	
84. <input type="checkbox"/> Not Approved for Release	
85. <input type="checkbox"/> Not Approved for Release	
86. <input type="checkbox"/> Not Approved for Release	
87. <input type="checkbox"/> Not Approved for Release	
88. <input type="checkbox"/> Not Approved for Release	
89. <input type="checkbox"/> Not Approved for Release	
90. <input type="checkbox"/> Not Approved for Release	
91. <input type="checkbox"/> Not Approved for Release	
92. <input type="checkbox"/> Not Approved for Release	
93. <input type="checkbox"/> Not Approved for Release	
94. <input type="checkbox"/> Not Approved for Release	
95. <input type="checkbox"/> Not Approved for Release	
96. <input type="checkbox"/> Not Approved for Release	
97. <input type="checkbox"/> Not Approved for Release	
98. <input type="checkbox"/> Not Approved for Release	
99. <input type="checkbox"/> Not Approved for Release	
100. <input type="checkbox"/> Not Approved for Release	

ELECTRONIC STRUCTURE OF GRAIN BOUNDARIES AND INTERFACES IN POLYCRYSTALLINE ZINC OXIDE

M. H. SUKKAR, H. L. TULLER, AND K. H. JOHNSON

Department of Materials Science and Engineering, M.I.T., Cambridge, Massachusetts

ABSTRACT

Preliminary theoretical models for the electronic structure of grain boundaries and interfaces in polycrystalline ZnO have been constructed on the basis of self-consistent-field X-alpha scattered-wave (SCF-X α -SW) cluster molecular-orbital calculations. The disposition and character of the interface states, relative to the valence and conduction bands of the otherwise perfect crystalline material, have been studied for clusters representing coordinatively unsaturated Zn surface sites and molecular O₂ chemisorption thereon. The possible effects of the resulting interface states on electron transport at grain boundaries in ZnO varistors have been addressed.

INTRODUCTION

Electronic ceramics whose properties are largely controlled by grain boundary phenomena have received a good deal of attention in recent years. One such device, the ZnO-based varistor, which is resistive at low voltages, "breaks down" at higher voltages (hundreds of volts/cm) to give a highly nonohmic regime in which the current-voltage relation is described by a power law, $I = kV^\alpha$ ($\alpha > 1$). Early models [1] attempted to ascribe the nonlinear varistor action to the existence of second-phase layers of insulating material separating the semiconducting grains. Recent high resolution transmission electron microscopy [2] shows, however, this not to be the case. Although a considerable number of alternative models have been proposed in recent years [3,4] they all propose in common the existence of a charged grain boundary interface bounded by space charge layers penetrating into the adjoining grains. All models either implicitly or explicitly rely on the existence of low-lying interface states or traps at the intergranular layers to provide for the formation of the potential barrier at the grain/grain-boundary interface. In particular, the recent models of Pike and Seager [5] quantitatively derive expressions for the temperature and voltage dependence of the potential barrier with the density-of-states function of the interfacial traps serving as a key parameter. The purpose of our investigation is to examine the nature of the electronic structure of ZnO surfaces and interfaces from first principles, and subsequently to attempt to relate our findings to experimental observations. This paper serves as our first effort in this direction.

Zinc oxide which forms in the wurtzite structure possesses a band gap energy of ~ 3.3 eV at room temperature. It can nevertheless be made highly semiconducting (n-type) either by heating in a reducing atmosphere to obtain an excess of Zn or by doping with donor impurities (e.g. Al). Under these conditions donor ionization energies are reported to be low (~ 0.05 eV), while electron mobilities are typically ~ 200 cm²/V-sec at 300°K. Acceptor impurities (e.g. Li), on the other hand, can drop the conductivity of these materials many orders of magnitude. Likewise, annealing ZnO in oxygen can be expected to have a similar

effect [6]. In the following analysis we examine in some detail the effects of excess oxygen on ZnO interfaces but limit our discussion to the nature of the interface states and how they are modified upon chemisorption of oxygen.

THE SCF- $X\alpha$ -SW CLUSTER MOLECULAR-ORBITAL METHOD

The inherently local nature of the ZnO grain boundary problem, coupled with the importance of chemical bonding (e.g. oxygen chemisorption) at the grain boundary interface, make traditional reciprocal (k)-space band-theoretical methods of solid state physics both inappropriate and impractical for determining grain-boundary electronic structure/properties relationships. Real-space molecular-orbital theory is more appropriate for this problem because it focuses on the electronic structure of a small cluster of atoms which simulates the local environment of the grain boundary. The feasibility of this approach is shown by the successful modeling of sulfur embrittlement of nickel grain boundaries by Messmer et al [7] using the SCF- $X\alpha$ -SW cluster molecular-orbital method [8].

The theoretical formalism and computational procedure underlying the SCF- $X\alpha$ -SW molecular-orbital method have been thoroughly documented elsewhere [8]. It is sufficient to summarize here that in applying this technique to grain boundaries in ZnO, appropriate clusters of atoms are chosen which are models for the local arrangement of atoms at the grain boundary interface. Each cluster is partitioned into: I. atomic, II. interatomic, and III. extramolecular regions of spherically and volume averaged potentials, including the $X\alpha$ approximation to electron-electron exchange and correlation, based initially on free-atom and free-ion $X\alpha$ potentials. Schrödinger's equation is then solved numerically in a composite partial-wave representation throughout regions I, II, and III, and the solutions along with their first derivatives are joined continuously via scattered-wave theory across the spherical boundaries separating these regions. These continuity conditions determine the cluster molecular-orbital wavefunctions, and their associated energy levels, which are then occupied with electrons according to the Pauli principle and Fermi statistics. From the occupied orbital wavefunctions, a new electronic charge density is calculated which, in turn, is used to construct a new potential throughout the cluster, and Schrödinger's equation is again solved for a new set of molecular-orbital wavefunctions and energy levels. This entire process is iterated until self-consistency of the electronic energy levels and charge distributions is attained. The procedure has been programmed for rapid computation on a digital computer.

PRELIMINARY THEORETICAL MODEL

The rectifying behavior of ZnO surfaces (electroded with Pt) exposed to oxygen, which disappears when heated to $\sim 600^\circ\text{K}$ in a vacuum and reappears when O_2 is reintroduced [9], strongly suggests a direct correlation between excess oxygen at ZnO interfaces and nonlinear I-V characteristics. This correlation is further supported by the disappearance of the nonlinear I-V characteristics of ZnO varistor materials upon annealing in a reducing atmosphere [10].

In order to provide a theoretical basis for this correlation, preliminary SCF- $X\alpha$ -SW molecular-orbital calculations of the type described in the preceding section have been carried out respectively for molecular O_2 and ZnO_3^{4-} and $\text{O}_2\text{ZnO}_3^{4-}$ clusters. The O_2 molecule calculations were carried out in order to (1) estimate the positions of chemisorbed O_2 levels with respect to the bulk ZnO levels and (2) enable a comparison of the occupation of its energy levels before and after chemisorption on ZnO surfaces. The ZnO_3^{4-} cluster was chosen as an initial model for ZnO free surfaces because of its simplicity and its preservation of underlying bulk character. This cluster may be thought of as representing either (1) a coordinatively unsaturated Zn site on a (0001) Zn

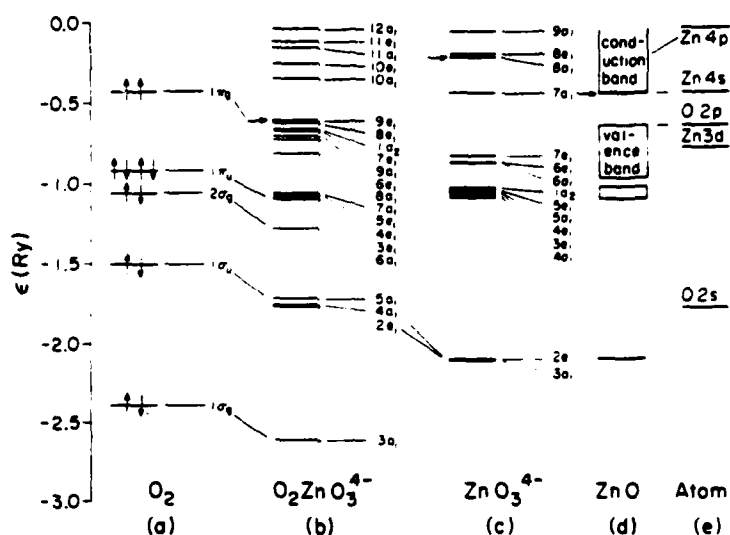


Fig. 1. SCF-X α -SW energy levels for (a) an O_2 molecule, (b) an $O_2ZnO_3^{4-}$ cluster, (c) a ZnO_3^{4-} cluster, (d) bulk (n-type) ZnO, and (e) the free Zn and O atoms. The highest occupied levels (the "Fermi levels") at $T = 0^\circ K$ are indicated by the horizontal arrows.

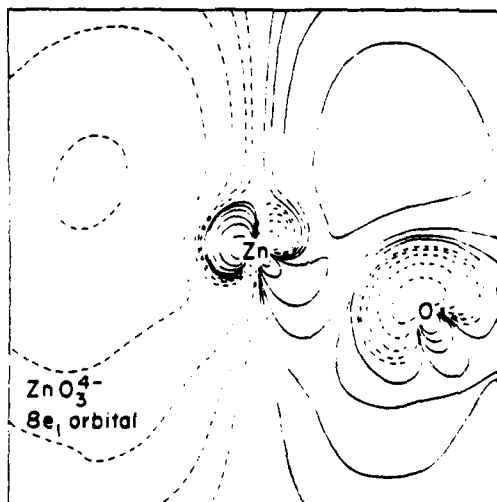


Fig. 2. Contour map for the $8e_1$ molecular-orbital wavefunction of a ZnO_3^{4-} cluster. The solid and dashed contours represent opposite phases of the wavefunction.

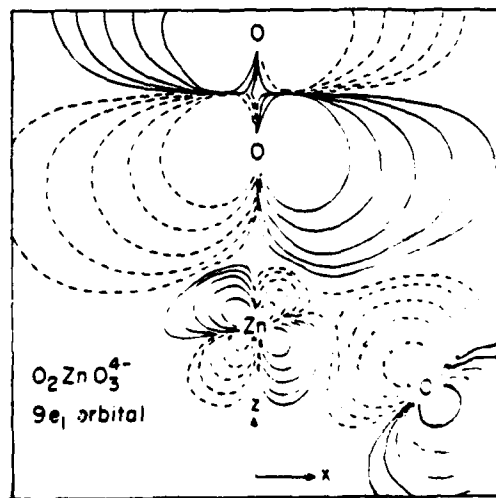


Fig. 3. Contour map for the $9e_1$ molecular-orbital wavefunction of an $O_2ZnO_3^{4-}$ cluster. The solid and dashed contours represent opposite phases of the wavefunction.

surface, (2) a step site on a {10T0} prismatic surface, (3) an oxygen vacancy on a (000T) O surface, or (4) a bulk oxygen vacancy. The O_2ZnO_3 cluster represents an O_2 molecule chemisorbed on the coordinatively unsaturated ZnO_3 cluster, with the O_2 molecular axis perpendicular to the plane formed by the three oxygens. This choice of O_2 orientation was made to preserve the C_{3v} point group symmetry of the ZnO_3 cluster, although preliminary calculations for O_2 oriented "parallel" to the surface indicate that the main conclusions about the effects of O_2 chemisorption on interface electronic structure are unaltered. These clusters are not large enough to distinguish between various ZnO surfaces or between unsaturated Zn surface sites on a (0001) surface and surface oxygen vacancies or steps. Nevertheless, it is felt that the study of the electronic structures of these simpler clusters is a necessary first step toward understanding grain boundary electronic structure and oxygen incorporation therein. The resulting cluster energy levels are shown in Fig. 1, where they are compared directly with the SCF- $X\alpha$ orbital energies for the O_2 molecule and Zn and O atoms. The levels are labeled according to the irreducible representations of the appropriate (e.g. C_{3v}) symmetry groups, and the highest occupied levels (the "Fermi levels") at absolute zero temperature are indicated by horizontal arrows. The electron spin occupancy of the O_2 molecular-orbital energy levels is indicated. Also shown schematically for comparison is the bulk ZnO band structure, which has been successfully modeled by previous SCF- $X\alpha$ -SW molecular-orbital calculations for a ZnO_6 cluster representing the nearest-neighbor environment in the bulk material [11]. The coincidence of the Fermi level with the bottom of the conduction band, as indicated by the arrow, denotes the usual n-type material.

It is found that a coordinatively unsaturated Zn surface site (or surface oxygen vacancy), as simulated by the ZnO_3 cluster, produces occupied states in the lower part of the otherwise unoccupied Zn s,p-like conduction band of intrinsic bulk ZnO. The predominantly Zn 4p-like character of the highest occupied of these conduction-band states, spatially directed away from the surface Zn site and antibonding with respect to the O_2p orbitals, is clearly visible in the wavefunction contour map for the thermally occupied ($T \sim 300^\circ K$) $8e_1$ orbital of the ZnO_3 cluster, plotted in the X-Z plane of the Zn atom and a nearest-neighbor O atom. Because of the embedding of these surface states in the conduction band, they function as electron donors, consistent with the n-type behavior of oxygen vacancies in ZnO.

Along with the s,p-like surface states in the conduction band, the antibonding Zn(3d)-O(2p) character in the otherwise primarily O(2p)-like valence band is significantly enhanced by the coordinative unsaturation. This enhanced Zn(3d) character in the valence band can also be interpreted as surface states and may be a major contribution to the well known catalytic activity of ZnO surfaces. The presence of surface states in both the conduction and valence band and absence of such states in the band gap are consistent with previous experimental [12-14] and theoretical [15] findings.

The calculated electronic structures of O_2 before and after chemisorption on a ZnO surface, as represented by the molecular-orbital energies of O_2 and O_2ZnO_3 in Fig. 1(a) and 1(b), respectively, indicate that there is indeed a net transfer of approximately one electron to the O_2 molecule upon chemisorption, as suggested in the literature [16]. Over the temperature range, $300^\circ K \lesssim T \lesssim 700^\circ K$, for which non-dissociative O_2 chemisorption (as distinguished from O_2 physisorption for $T \lesssim 300^\circ K$) on ZnO is believed to occur [16], the present theoretical model suggests that thermally populated "surface states" embedded in the conduction band [e.g. the $8e_1$ orbital in Fig. 1(c) for the representative ZnO_3 cluster], and having the spatially localized Zn $4p\pi^*$ character shown in Fig. 2, effectively transfer one electron per coordinatively unsaturated Zn surface site to each O_2 molecule through symmetry conserving overlap with the half empty O_2 $1\pi_g$ molecular orbital shown in Fig. 1(a). This elec-

tron transfer, followed by considerable orbital rehybridization within the valence band at the O_2 -ZnO interface, results in an empty conduction band and partially occupied $O_2 \pi^*$ -like states coinciding with the top of the valence band. The latter states are represented by the $9e_1$ orbital of the model O_2ZnO_3 cluster in Fig. 1(b) having the orbital topology shown in Fig. 3. Note also in Fig. 1(b) the one-to-one correspondence between the various O_2 bonding molecular-orbital energy levels below the 1π level and energy levels of the O_2ZnO_3 cluster lying well below the top of the valence band, consistent with the assumption of non-dissociative O_2 chemisorption on ZnO. The presence of partially empty $O_2 \pi^*$ -like states of the type shown in Figs. 1(b) and 3 at the top of the valence band implies p-type ("hole") character at the O_2 -ZnO interface, in distinct contrast to the n-type ("electron") character of the bulk and surface electronic structures of ZnO shown in Figs. 1(d) and 1(c), respectively. This dramatic change from n to p character when occupied electronic states in the conduction band are compensated for by O_2 chemisorption, assuming continuity of the Fermi energy, reflects the Schottky-barrier-like "band bending" that is believed to occur at the grain boundaries in ZnO varistors [3-5]. The possible role of the $O_2 \pi^*$ -like hole states at the top of the valence band at an O_2 -ZnO interface as intergranular electron "trapping" states responsible for the rapid increase of electric current with applied voltage in ZnO varistors [3-5] is currently under theoretical investigation using the SCF-X α -SW cluster molecular-orbital method.

ACKNOWLEDGMENTS

We are grateful to the Office of Naval Research for supporting this research.

REFERENCES

1. K. Eda, J. Appl. Physics 49, 2964 (1978).
2. D. R. Clarke, J. Appl. Phys. 49, 2407 (1978).
3. J. D. Levine, Crit. Rev. Solid State Sci. 5, 597 (1975).
4. P. R. Emtage, J. Appl. Phys. 48, 4372 (1977).
5. G. E. Pike and C. H. Seager, J. Appl. Phys. 50, 3414 (1979).
6. K. I. Hagemark and L. C. Chacka, J. Solid St. Chem. 15, 261 (1975).
7. C. L. Briant and R. P. Messmer, Phil. Mag. 42B, 569 (1980).
8. J. C. Slater and K. H. Johnson, Phys. Rev. 85, 844 (1972); K. H. Johnson, in Advances in Quantum Chemistry, Vol. 7, edited by P. O. Lowdin (Academic, New York, 1973), p. 143; J. C. Slater and K. H. Johnson, Physics Today 27, 34 (1974); J. C. Slater, The Self Consistent Field for Molecules and Solids, Vol. 4 of Quantum Theory of Molecules and Solids (McGraw-Hill, New York, 1974), p. 101; K. H. Johnson, in Annual Review of Physical Chemistry, Vol. 26, edited by H. Eyring, C. J. Christensen, and H. S. Johnston (Annual Reviews, Palo Alto, 1975); p. 39.
9. G. Heiland, Z. Phys. 148, 15 (1957).
10. F. A. Selim et al., J. Appl. Phys. 51, 765 (1980).

11. J. M. Kowalski, M.S. Thesis, Department of Materials Science and Engineering, June, 1978 (unpublished).
12. W. J. Gopel, J. Vac. Sci. Technol. 16, 1229 (1979).
13. J. F. Dewald, Bell Syst. Tech. J. 39, 615 (1960).
14. H. G. Gatos and J. Lagowski, J. Vac. Sci. Technol. 10, 130 (1973).
15. I. Ivanov and J. Pollmann, Solid State Commun. 36, 361 (1980).
16. See, For example, W. Gopel and U. Lampe, Phys. Rev. B22, 6447 (1980).

DA
FIL